J. Fluid Mech. (2004), *vol.* 498, *pp.* 113–121. © 2004 Cambridge University Press
DOI: 10.1017/S0022112003006955 Printed in the United Kingdom

A scheme for micro-manipulation based on capillary force

By KENICHI J. OBATA, TOMOYUKI MOTOKADO, SHIGEKI SAITO AND KUNIO TAKAHASHI

Department of International Development Engineering, Graduate School of Science and Engineering, Tokyo Institute of Technology, O-okayama, Meguro-ku, Tokyo 152-8552, Japan

(Received 23 May 2003 and in revised form 30 September 2003)

As the size of object diminishes, the effect of adhesional forces grows stronger for micro-manipulation and so. The capillary force generated by a liquid bridge can be greater than both the capillary force generated by another bridge and the adhesional force because the capillary force can be controlled by regulation of the liquid volume. We propose a micro-manipulation method based on the regulation of liquid bridge volume. A numerical investigation to estimate the capillary force from a given liquid volume is also presented, and four phases of capillary force curves are obtained from it. If an object is supported by two liquid bridges, we can predict which bridge collapse by a stability analysis for the wide range of liquid volume using the force curve.

1. Introduction

In micro-manipulation, the influence of gravitational force is extremely small compared to adhesional force. Thus, in order to perform reliable micro-manipulation, we need to use a force that is both controllable and greater than the adhesional force. Saito, Miyazaki & Sato (2002*a*) and Saito *et al.* (2002*b*) have analysed the mechanical force required to slip and roll an object by considering the adhesional effect, using a scanning electron microscope, and proposed a method of manipulation using a needle shaped tool. If the required force is large and compressive, however, their method might break a brittle object because of high stress imparted by the tool. Takahashi *et al.* (2001) have evaluated the force generated by Coulomb interaction and estimated the voltage required to detach an adhered particle. If the required voltage is too large, Takahashi *et al*'s method might cause electric discharge and melting of the object (see Saito, Himeno & Takahashi 2003). Tanikawa, Hashimoto & Arai (1998) have picked/placed an object with a micro-hand and a micro-drop, but they have not provided any analysis of the capillary force involved.

As shown by Tanikawa *et al.* (1998), the capillary force is large enough to detach an adhered particle if the liquid has volume sufficiently smaller than that of the particle. This indicates the possibility of controlling the capillary force by means of regulation of the liquid volume. We propose a micro-manipulation method based on this idea. Figure 1 shows our proposed procedure for micro-manipulation. (I) A probe with a known volume of liquid is located above a spherical object on a substrate. (II) The probe comes down to form a liquid bridge between the probe and the object. Consequently, capillary force F_p is generated on the object. (III) The probe is lifted up, and the object is picked up by means of the capillary force. (IV) The probe is positioned above a target point on which a micro-drop has been applied.

https://doi.org/10.1017/S0022112003006955 Published online by Cambridge University Press

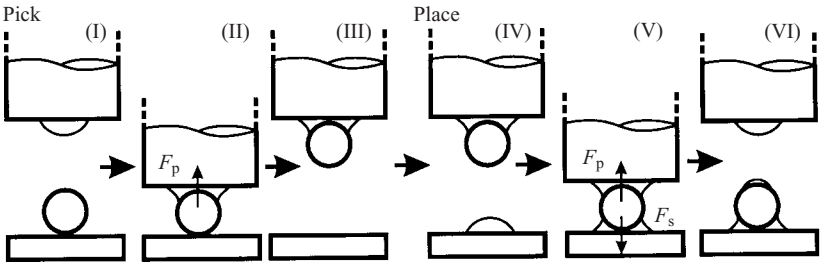


FIGURE 1. Schematic illustration of pick/placing procedure: (I) positioning, (II) lowering, (III) picking up, (IV) positioning, (V) lowering, (VI) placing.

(V) The object held by the probe is lowered to form another liquid bridge between the substrate and the object. Therefore, capillary force F_s is also generated on the object. (VI) The probe is pulled up in order to collapse the probe–object liquid bridge. The object is thus put on the substrate.

In this model, the probe–object liquid bridge must collapse before the object–substrate bridge during the operations (V) and (VI). We investigate the conditions of liquid bridge stability, and in particular the force required to collapse the liquid bridge. The object can be picked/placed by controlling F_p and F_s.

The profile of the liquid bridge is usually calculated through the circle approximation (see Gao, Tian & Bhushan 1995; Israelachvili 1985; Pitois, Moucheront & Chateau 2001) and the capillary force is estimated from the profile. The approximation is only valid for sufficiently small volume of the liquid compared to the volume of the object. Erle, Gillette & Dyson (1970) have shown the limit of stability as the volume of a liquid bridge between two disks having a fixed separation is reduced. Although a detailed analysis has been presented by Gillette & Dyson (1971) and Gaudet, McKinley & Stone (1996) have given an analysis of bridge stability which is similar to ours, they were not considering manipulation with liquids, and furthermore, they did not take into account effects of contact angles because the inclination of a meniscus can change freely at the edge of a disk. Orr, Scriven & Rivas (1975) have solved the Laplace–Young equation analytically in terms of elliptic integrals, but no direct solution for a given conserved value of the liquid volume can be obtained from it. Zhang, Padgett & Basaran (1996) have presented the limit value of bridge length between two solid disks that are separating at a constant velocity. Padday *et al.* (1997) have found the liquid volume required for breakage of pendant drops supported underneath by a solid endplate both numerically and experimentally. Zhang *et al.* (1996) and Padday *et al.* (1997) take account of viscosity in discussing the dynamic collapse of the liquid bridge; however, the statistical force required to collapse a liquid bridge between two solids has not been clearly investigated so far.

In the present paper, a numerical investigation is presented and applied to evaluate the force required to collapse a liquid bridge at a given value of the liquid volume based on Orr *et al.*'s work. The force required can be calculated for a wide range of liquid volume. Capillary force curves are obtained and the stability of the liquid bridge is discussed in terms of them. Although a numerical method is used, all the parameters are normalized and a systematic evaluation is carried out. We propose a procedure for a micro-manipulation scheme using capillary force controlled by regulating the liquid volume. Note that we are not concerned here with any mechanical problems of the liquid flow to the surface of the manipulation probe or substrate.

https://doi.org/10.1017/S0022112003006955 Published online by Cambridge University Press

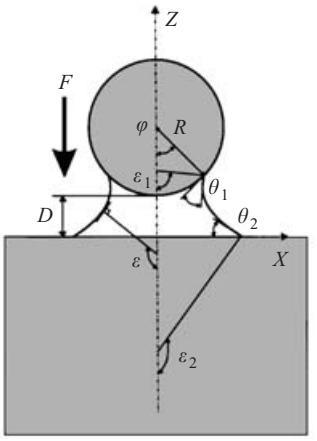


FIGURE 2. Liquid bridge between a spherical object and a plate.

2. Analysis of the liquid bridge

2.1. *Geometrical properties*

Figure 2 shows a model for the analysis of a liquid bridge between a spherical object and the plate of a probe or a substrate, where R is the radius of the object, D is the distance from the plate to the object, φ is the filling angle of the object, F is the attractive force acting on the object, and V is the volume of the liquid between two solids. The meniscus forms contact angles θ_1 at the object and θ_2 at the plate. We make the following assumptions. (i) The influence of gravity is negligible, i.e. the Bond number ($gL^2\Delta\rho/\sigma$, where g is the local acceleration due to gravity, $\Delta\rho$ the density difference between the fluids on either side of the interface, and L some characteristic length for the system) is sufficiently small (see Orr *et al.* 1975). (ii) The dynamic flow of the liquid is negligible. (iii) The volume of the liquid is conserved. (iv) The contact angles are determined by Young's equation (see Israelachvili 1985). (v) The object and the plate are rigid. (vi) The area of the plate is infinite.

The stability profile of the liquid bridge can be obtained from Young–Laplace equation (see Orr *et al.* 1975), which relates the hydrostatic pressure difference to the local mean curvature H and surface tension σ:

$$\Delta P = 2H\sigma, \tag{2.1}$$

where ΔP is the pressure difference between inside and outside the liquid. Since ΔP is a constant, the surface of the meniscus has the same mean curvature at any local point. The value of H in (2.1) can be expressed with geometrical parameters as

$$2H = \frac{\mathrm{d}^2Z/\mathrm{d}X^2}{[1+(\mathrm{d}Z/\mathrm{d}X)^2]^{3/2}} + \frac{\mathrm{d}Z/\mathrm{d}X}{X[1+(\mathrm{d}Z/\mathrm{d}X)^2]^{1/2}}, \tag{2.2}$$

where X and Z are cylindrical coordinates in figure 2, i.e. the surface profile of the meniscus. The first term is meridional curvature and the second term is azimuthal curvature of the meniscus surface. With the following normalization:

$$z = \frac{Z}{R}, \quad x = \frac{X}{R}, \quad d = \frac{D}{R}, \quad f = \frac{F}{\pi R\sigma}, \quad v = \frac{V}{R^3}, \tag{2.3}$$

https://doi.org/10.1017/S0022112003006955 Published online by Cambridge University Press

Normalized mean curvature	Parameter c	Meridional curvature	Sign
$2HR < 0$	+		−
$0 < 2HR < \dfrac{2\sin\varepsilon_1}{x_1}$	−	+	+
$0 < 2HR < \dfrac{2\sin\varepsilon_1}{x_1}$	−	−	−
$\dfrac{2\sin\varepsilon_1}{x_1} < 2HR$	+		+

TABLE 1. The choice of signs in (2.6) and (2.7).

(2.2) can be written as

$$2HR = \frac{\mathrm{d}(\sin\varepsilon)}{\mathrm{d}x} + \frac{\sin\varepsilon}{x}, \tag{2.4}$$

where ε is the angle between the normal to the meniscus and the vertical axis. Since the left-hand side of this equation is constant, it can be solved as a two-point boundary-value problem, for which the boundary conditions are the inclinations of the menisci on the solid surfaces. These inclinations are determined by the slopes of the solid surfaces and the respective contact angles θ_1 and θ_2 (see figure 2). Thus, the boundary conditions are expressed by

$$\left.\begin{aligned} &\varepsilon_1 = \theta_1 + \varphi, \quad z_1 = d + 1 - \cos\varphi, \quad x_1 = \sin\varphi, \\ &\varepsilon_2 = \pi - \theta_2, \quad z_2 = 0. \end{aligned}\right\} \tag{2.5}$$

The boundary-value problem has the solution (see Orr *et al.* 1975)

$$x = \frac{\sin\varepsilon \mp (\sin^2\varepsilon + c)^{1/2}}{2HR}, \tag{2.6}$$

$$z = \int_{\varepsilon_2}^{\varepsilon} \frac{(\sin^2\varepsilon + c)^{1/2} \mp \sin\varepsilon}{2HR(\sin^2\varepsilon + c)^{1/2}} \sin\varepsilon \,\mathrm{d}\varepsilon, \tag{2.7}$$

where c is a constant parameter defined as

$$c \equiv (2HR)^2 x_1^2 - 2(2HR)x_1 \sin\varepsilon_1. \tag{2.8}$$

The choice of signs in (2.6) and (2.7) is determined by the value of the normalized mean curvature $2HR$, the parameter c, and the meridional curvature (see table 1).

Then, the normalized liquid volume v and the normalized distance d can be described in terms of the integral of ε:

$$v = \int_{z_2}^{z_1} \pi x^2 \,\mathrm{d}z = \int_{\varepsilon_2}^{\varepsilon_1} \pi x^2 \frac{\mathrm{d}z}{\mathrm{d}\varepsilon} \,\mathrm{d}\varepsilon \tag{2.9}$$

and

$$d = z_1 - (1 - \cos\varphi). \tag{2.10}$$

2.2. *Capillary force*

The static attractive force due to the meniscus is the sum of the pressure difference and the axial component of the surface tension acting on the object (see Orr *et al.* 1975):

$$F = 2\pi R\sigma[\sin\varphi \sin(\theta_1 + \varphi) - HR\sin^2\varphi]. \tag{2.11}$$

https://doi.org/10.1017/S0022112003006955 Published online by Cambridge University Press

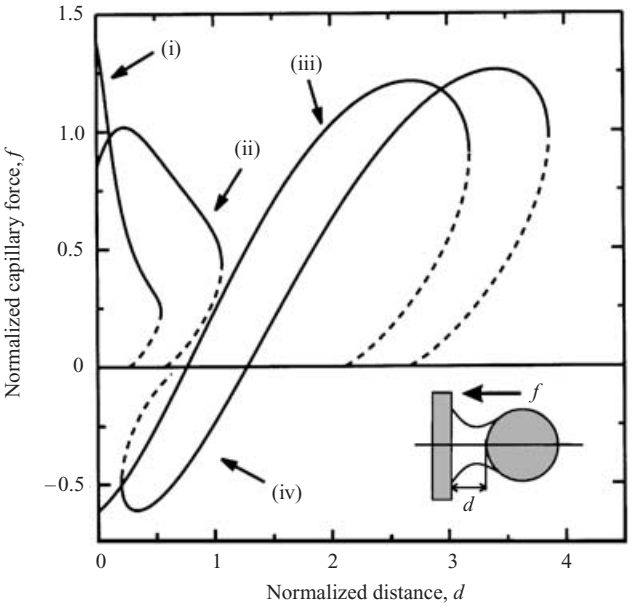


FIGURE 3. Capillary force curves ($\theta_1 = \theta_2 = 60°$): (i) $v = 0.1$, (ii) $v = 1.0$, (iii) $v = 50.0$, (iv) $v = 100.0$.

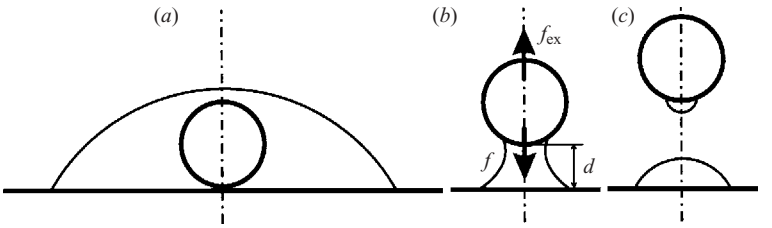


FIGURE 4. Schematic illustration of the liquid profile and the definition of the distance d, the capillary force f, and the external force f_{ex}: (a) the object is fully covered with the liquid; (b) the liquid bridge; (c) after collapse of the liquid bridge.

From (2.3), the normalized capillary force can be obtained as

$$f = 2[\sin\varphi \sin(\theta_1 + \varphi) - HR \sin^2\varphi]. \tag{2.12}$$

3. Capillary force curve

3.1. *Phases of the force curve*

The solid lines in figure 3 show the capillary force f as a function of the distance d for different values of v and $\theta_1 = \theta_2 = 60°$. The broken lines obtained from (2.4), (2.10), and (2.12) are the imaginary solution of the present problem. Each curve exhibits the different features of the liquid bridge: (i) The capillary force is always attractive, and the value of f decreases with d. (ii) The capillary force is always attractive, and f has a maximum value. (iii) The capillary force is repulsive for $d = 0$, and f has a maximum value, and is zero at a certain point. (iv) The liquid bridge cannot exist for $d = 0$. In this case, the object is fully covered with the liquid, as shown in figure 4(a). The capillary force is repulsive for the minimum d, and f reaches a minimum and

https://doi.org/10.1017/S0022112003006955 Published online by Cambridge University Press

then increases with d until reaching a maximum value. The value of f is zero at a certain point. When $f=0$, the object floats on the liquid; such floating can be observed in cases (iii) and (iv).

3.2. *Stability of the liquid bridge*

The liquid bridge is treated as static. Thus the capillary force curve is just plotted in its stable equilibrium state, and indicates the range of distances where the liquid bridge can exist statically, and also shows the value of the external force f_{ex} that would equilibrate the capillary force (see figure 4*b*). If the distance d is above the range of the curve, the liquid bridge cannot exist as in figure 4(*b*) and it must collapse as in figure 4(*c*). If the distance d is below the range of the curve, figure 4(*b*) does not apply and the object is fully covered with liquid as in figure 4(*a*). If the force f_{ex} is larger than the maximum value of the curve, the liquid bridge is extended until eventually the bridge collapses (see Padday *et al.* 1997).

3.3. *Application to micro-manipulation*

In the micro-manipulation method, F_p and F_s are acting on the object. In order to keep a stable equilibrium, $f_p(\equiv F_p/\pi R\sigma)$ must be equal to $f_s(\equiv F_s/\pi R\sigma)$. If f_p is greater than f_s, the object is attracted to the probe and tends to maintain the stability of the bridge; however, if f_p is greater than the maximum value of f_s, the bridge on the substrate can be elongated and collapse. Therefore, we can predict which liquid bridge will collapse: if the maximum value of f_p is larger than f_s, the object–substrate bridge must collapse; if the maximum value of f_s is larger than f_p, the probe–object bridge must collapse.

Figure 5 shows the dependence of the maximum capillary force f_{max} on the liquid volume v for $\theta=\theta_1=\theta_2$. The solid lines represent the control of the maximum capillary force by the regulation of the liquid volume. The dashed lines show the thresholds of the phases of the force curve.

3.4. *Comparison to adhesional force*

The adhesional effect must be taken account in the micro-manipulation. The adhesional force $F_{adh.}$ is expressed as

$$F_{adh.} = \tfrac{3}{2}\pi R\Delta\gamma, \tag{3.1}$$

where $\Delta\gamma$ is the work required for adhesion of interface between two solids (see Johnson *et al.* 1971). It can be normalized as

$$f_{adh.} = \frac{F_{adh.}}{\pi R\sigma}. \tag{3.2}$$

If the normalized capillary force f is greater than $\frac{3}{2}\Delta\gamma/\sigma$, the object can be removed from the substrate.

4. Manipulation procedure

4.1. *Picking procedure*

In order to pick up the object during the manipulation, (II) and (III) in figure 1, F_p must be greater than $F_{adh.}$. If $\Delta\gamma=0.1\,\mathrm{N\,m^{-1}}$ and the liquid is water ($\sigma=0.072$), the normalized adhesional force $f_{adh.}$ is 2.08. The liquid volume on the probe v_p must be regulated in order to exceed the adhesional force. Figures 6(*a*) and 7(*a*) show examples of how to determine the liquid volume on the probe v_p. The capillary force

https://doi.org/10.1017/S0022112003006955 Published online by Cambridge University Press

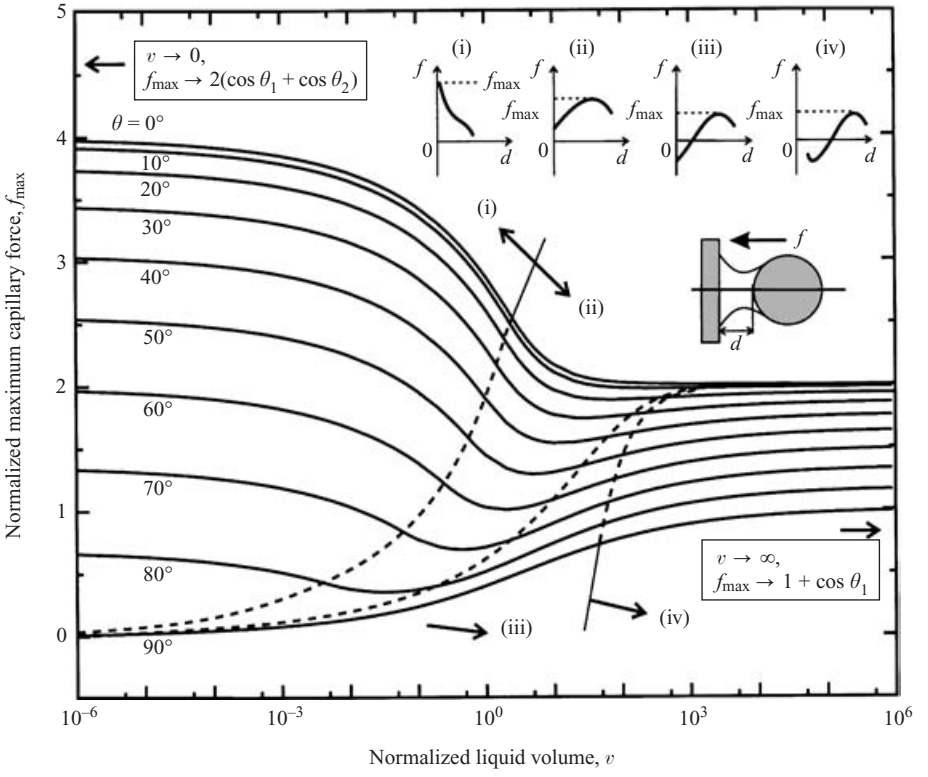


FIGURE 5. Relation between the liquid volume and the maximum capillary force (solid lines), and the threshold for the phases of the force curve ($f = F/\pi R\sigma$, $v = V/R^3$) (dashed lines), for $\theta = \theta_1 = \theta_2$. (i) f_{max} occurs for $d = 0$. (ii) f_{max} occurs for $d > 0$. (iii) $f < 0$ for $d = 0$. (iv) The liquid bridge cannot exist for $d = 0$.

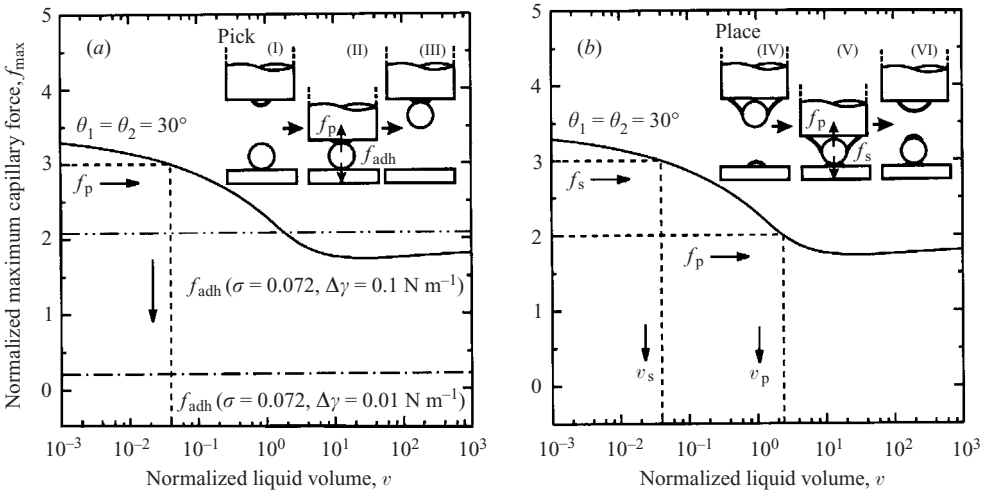


FIGURE 6. Determination of liquid volume v_p and v_s required in order to manipulate the object ($\theta = 30°$): (*a*) pick; (*b*) place.

https://doi.org/10.1017/S0022112003006955 Published online by Cambridge University Press

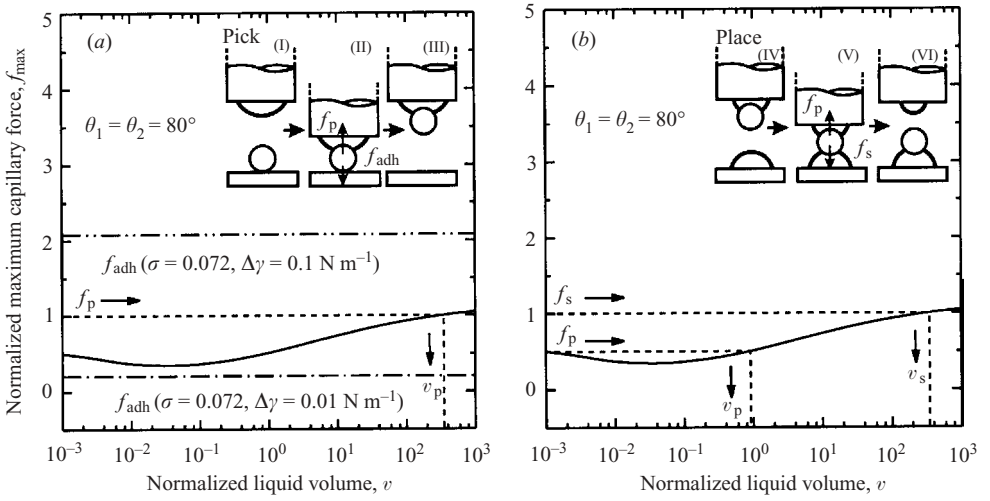


FIGURE 7. Determination of liquid volumes v_p and v_s required in order to manipulate the object ($\theta = 80°$): (*a*) pick; (*b*) place.

f_p should be set to be greater than the adhesional force $f_{adh.}$. The liquid volume v_p required for the picking manipulation can be obtained from these diagrams.

4.2. *Placing procedure*

If the phase of the force curve is (i) or (ii) in figure 5 in terms of the probe–object liquid bridge, the adhesional force acts on the object. In this case, in order to simplify the discussion, we assume that solid–solid contact occurs at both the probe–object and the object–substrate interface. Then, the adhesional forces acting on both sides of the object can be cancelled. Thus, successful manipulation depends just on the difference between f_p and f_s. Furthermore, the adhesional force is expected to be negligible when the contact point is covered with the liquid, from Dupre's equation (see Israelachvili 1985). In cases (iii) and (iv), because the object floats, no adhesional force acts on the object. Thus, in all cases, the placing manipulation is discussed in terms of the difference between the capillary forces.

For the placing manipulation, the probe–object bridge must collapse. Thus we need to regulate the liquid volumes v_p and v_s so that the maximum value of f_s is greater than that of f_p.

Figures 6(*b*) and 7(*b*) show examples of how to determine the liquid volume on the probe v_p and on the substrate v_s. The capillary force f_s must be set to be greater than f_p. The liquid volumes v_p and v_s required for the placing manipulation can be obtained from these diagrams.

4.3. *Effect of contact angles*

There are two differences between figures 6 and 7. The first is the volume required. The maximum force f_{max} decreases with v in figure 6, and it increases with v in figure 7. Thus, in the placing procedure, v_p should be greater than v_s for small contact angles and it should be smaller than v_s for large contact angles. The second is the phase of the capillary force curve. If the phase is (i) or (ii) as shown in figure 6, the capillary force is always attractive. Thus the object must form a solid–solid contact at the probe–object and/or the object–substrate interface. If the phase is (iii) or (iv) as shown in figure 7, the bridge has a length at which the capillary force

https://doi.org/10.1017/S0022112003006955 Published online by Cambridge University Press

is zero, i.e. the object floats. Therefore the probe can approach the object without causing mechanical damage. This indicates a great advantage of our method, because conventional methods for micro-manipulation can impart large stress to the object giving the possibility of damage.

5. Conclusion

A scheme for micro-manipulation based on the capillary force has been presented in terms of the regulation of liquid volume. The stability of the liquid bridge has been discussed in terms of the capillary force curve to collapse the liquid bridge. A numerical method to plot the force curve and its four phases have also been presented. The bridge can collapse due to the applied force being greater than the maximum capillary force. Smaller contact angle and liquid volume generate greater capillary force. For the manipulation, a mechanism that is able to supply small amounts of liquid needs to be developed.

The authors would like to express their sincere gratitude to Dr M. Urago for his kind and helpful discussion about the stability of the liquid bridge. This study was supported by a Grant-in-Aid for Scientific Research from the Ministry of Education, Culture, Sports, Science, and Technology.

REFERENCES

Erle, M. A., Gillette, R. D. & Dyson, D. C. 1970 Stability of interfaces of revolution with constant surface tension-the case of the catenoid. *Chem. Engng J.* **1**, 97–109.

Gao, C., Tian, X. & Bhushan, B. 1995 A meniscus model for optimization of texturing and liquid lubrication of magnetic thin-film rigid disks. *Tribology Trans.* **38**, 201–212.

Gaudet, S., McKinley, G. H. & Stone, H. A. 1996 Extensional deformation of Newtonian liquid bridges. *Phys. Fluids* **8**, 2568–2579.

Gillette, R. D. & Dyson, D. C. 1971 Stability of fluid interfaces of revolution between equal solid circular plates. *Chem. Engng J.* **2**, 44–54.

Israelachvili, J. 1985 *Intermolecular and Surface Forces*. Academic.

Johnson, K. L., Kendall, K. & Roberts, A. D. 1971 Surface energy and the contact of elastic solids. *Proc. R. Soc. Lond.* A **324**, 301–313.

Orr, F. M., Scriven, L. E. & Rivas, A. P. 1975 Pendular rings between solids: meniscus properties and capillary force. *J. Fluid Mech.* **67**, 723–472.

Padday, J. F., Petre, G., Rusu, C. G., Gamero, J. & Wozniak, G. 1997 The shape, stability and breakage of pendant liquid bridges. *J. Fluid Mech.* **352**, 177–204.

Pitois, O., Moucheront, P. & Chateau, X. 2001 Rupture energy of a pendular liquid bridge. *Eur. Phys. J.* B **23**, 79–86.

Saito, S., Himeno, H. & Takahashi, K. 2003 Electrostatic detachment of an adhering particle from a micromanipulated probe. *J. Appl. Phys.* **93**, 2219–2224.

Saito, S., Miyazaki, H. T. & Sato, T. 2002*a* Micro-object pick and place operation under sem based on micro-physics. *J. Robotics Mechatronics* **14**, 227–237.

Saito, S., Miyazaki, H. T., Sato, T. & Takahashi, K. 2002*b* Kinematics of mechanical and adhesional micromanipulation under a scanning electron microscope. *J. Appl. Phys.* **92**, 5140–5149.

Takahashi, K., Kajihara, H., Urago, M., Saito, S., Mochimaru, Y. & Onzawa, T. 2001 Voltage required an adhered particle by Coulomb interaction for micromanipulation. *J. Appl. Phys.* **90**, 432–437.

Tanikawa, T., Hashimoto, Y. & Arai, T. 1998 Micro drops for adhesive bonding of micro assemblies and making a 3-d structure "micro scarecrow". *Proc. IEEE Intl Conf. on Intelligent Robots and Systems* pp. 776–781.

Zhang, X., Padgett, R. S. & Basaran, O. A. 1996 Nonlinear deformation and breakup of stretching liquid bridges. *J. Fluid Mech.* **329**, 207–245.

https://doi.org/10.1017/S0022112003006955 Published online by Cambridge University Press